Indian J Phys
https://doi.org/10.1007/s12648-019-01570-z

ORIGINAL PAPER

Variable wavelength Newton's rings formed in transmission for measuring radius of curvature and sub-micrometric thin film thickness

I G Abd El-Sadek*, W A Ramadan, M Nawareg and A S El-Tawargy

Optics Research Group, Physics Department, Faculty of Science, Damietta University, New Damietta City 34517, Egypt

Received: 17 November 2018 / Accepted: 20 June 2019

Abstract: In this paper, Newton's rings interferometer was used for radius of curvature and sub-micrometric film thickness determination by varying the wavelength of the illuminating source. This was performed by using a partially reflecting spherical surface placed on a partially reflecting plane surface. The illuminating source was a halogen lamp followed by a monochromator in order to select a desired wavelength. By plotting a relation between values of wavelengths and rings' radii for different interference orders, the radius of curvature for the used spherical surface was retrieved. In addition, the system was used to determine the thickness of a sub-micrometric thin film. This was done by depositing the film on half of the glass plane surface. The step made by the presence of the film was employed in measuring the film's thickness. By measuring the rings' radii in both thin film and film-free regions for different interference orders and wavelengths, we succeeded in determining the film thickness by an accurate, simple and straightforward method with a nano-metric accuracy.

Keywords: Newton's rings interferometer; Radius of curvature; Sub-micrometric thin film thickness; Variable wavelength

PACS Nos.: 42.25.Hz; 06.20.−f; 42.15.−i

1. Introduction

Newton interferometer is one of the most important and oldest known interferometers. Simply, it is an arrangement of two surfaces kept in contact and is illuminated by a monochromatic source of light. The ordinary setup which was designed by Newton in 1730 is the most common technique used for quality control of optical surfaces and other important applications [1]. Due to its simplicity and high accuracy, this interferometric system attracted the attention of many research groups around the world. A short historical survey on the usage and the applications of Newton's rings system is given as follows.

Stern [2] presented a modified version of Newton's rings interferometer used for measuring thin film thickness. In this interferometer, a silvered lens is placed on a thin film with silver overlay. Gentle and Halsall [3] used Newton interferometer to determine Poisson's ratio of a polymeric sphere placed in contact with an optical plate.

Newton's rings were used to demonstrate the mean features of the spatial filtering theory by Dettwiller and CHavel [4]. Medhat et al. [5] introduced a powerful method based on Newton's rings for determining the surface parameters of aspheric lenses, i.e., astigmatism, asphericity, radius of curvature, surface topography, rotation asymmetry and the deviation of the shape from the theoretically stated ones. Dubrovskii et al. [6] proposed a new technique based on Newton's rings to measure the swelling pressure of a polymer gel. In this method, the gel swelling was used as a force-measuring diaphragm by putting it in a closed chamber with a flexible wall. The number of the rings formed between the diaphragm and the glass plate was used to determine the diaphragm deflection and then determining the swelling pressure.

Moreover, Newton's rings were used for coherence imaging by Podoleanu et al. [7]. They used some optical modifications in one arm of Michelson interferometer. The orthogonal galvo-scanning mirrors were used in the

*Corresponding author, E-mail: ibrahimsadek51@gmail.com; ibrahimsadek@du.edu.eg

Published online: 30 August 2019

formation of Newton's rings when the two interferometer arms were in match.

Illueca et al. [8] exploited Newton's rings for characterizing ophthalmic lenses. They used spherical and astigmatic lenses for the system calibration. Results showed that they measured the radii of curvature with an accuracy that varies between 0.3 and 0.7% for radii of curvature.

Newton's rings are also used in near-field optics. Goldner et al. [9] used these rings in near-field scanning microscopy and measuring the roughness of thin films. Wahl et al. [10] presented a new method employing Newton's rings analysis to measure thickness of a solid transferred film during in situ tribological studies. Raveesha et al. [11] used the Newton's ring interferometer to determine the radius of curvature of spherical surfaces based on the fact that the dark and bright fringes position can be used to measure the air-gap thickness at this point. Yang et al. [12] proposed a virtual method to measure the large radius of curvature for a spherical surface using Newton's rings phase-shifting interferometer. Their results showed that the measurement accuracy is better than 0.18% for a spherical mirror with a radius of curvature of 41,400 mm.

Wu et al. [13] presented an improved fractional Fourier transform (FRFT) to analyze Newton's rings and for retrieving the physical parameters of the used surface such as radius of curvature. Ramadan and Wahba [14] presented a simulation for ring fringes formed through spherical and plane reflecting surfaces. This method assumed that the fringes were formed according to the multiple reflections between the reflecting surfaces. In addition, they investigated the impact of image plane position, radius of curvature of the spherical surface and the distance between the plane and spherical surface on the fringes' intensity distribution.

According to the presented survey, one can notice that Newton's rings interferometer is usually used at reflection mode. In this work, it is used in transmission and we added the facility of varying the wavelength to be used for radius of curvature retrieving. In addition, we proposed a direct and quite accurate method for measuring the sub-micrometric thin film thickness using Newton's rings interferometer.

2. Theory

2.1. Spherical radius retrieving

When a lens is placed on a glass plate, a thin film of air with a variable thickness is enclosed between the lower and the upper surfaces of the lens and the glass plate, respectively. Due to the superposition of the optical rays passing through this arrangement, concentric fringes are produced which are known as Newton's rings. From the geometry of Fig. 1, the relation between the variable thin film's thickness t and a ring's radius r_n is given by Eq. (1),

$$t(r) = R - \sqrt{R^2 - r_n^2} \tag{1}$$

where R is the radius of curvature of the used convex lens and n is an integer that indicates the order of the interference rings.

Relation (1) can be approximated as:

$$t(r) \approx \frac{r_n^2}{2R} \tag{2}$$

In case of transmitted light, through the interferometer, and when the optical path difference equals an integer multiplication of a half wavelength, bright fringes can be obtained. It means that the condition of obtaining constructive interference could be written as,

$$t(r) = \frac{r_n^2}{2R} = n\frac{\lambda}{2} \tag{3}$$

where λ is the wavelength of the used monochromatic light. In case of varying wavelengths, the ring's radius varies consequently and Eq. (3) can be written as:

$$r_{n,}^2 = nR\lambda \tag{4}$$

From Eq. (4), a central bright fringe is formed at the contact point of the two surfaces, i.e., the position of interfered rays having equal path lengths. Moreover, this relation is a linear behavior between the wavelength λ and the squared value of the fringe radius $r_{n,}^2$ for each order of interference n. Experimentally, we can verify relation (4) to obtain different straight lines for different bright ring orders. It is obvious that the slopes (m_n) of these lines are equal to (n R), i.e.,

$$m_n = nR \tag{5}$$

Based on Eq. (5), a relation between the obtained slopes m_n and the order n can be plotted to obtain another straight

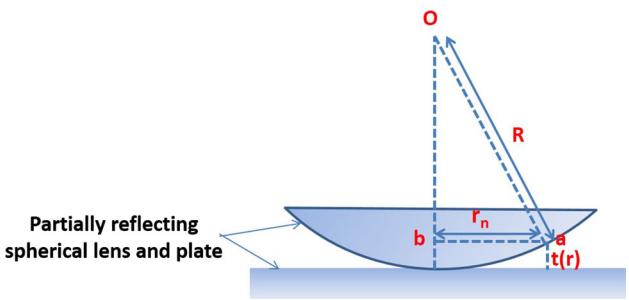

Fig. 1 A schematic diagram showing the used Newton's interferometer setup

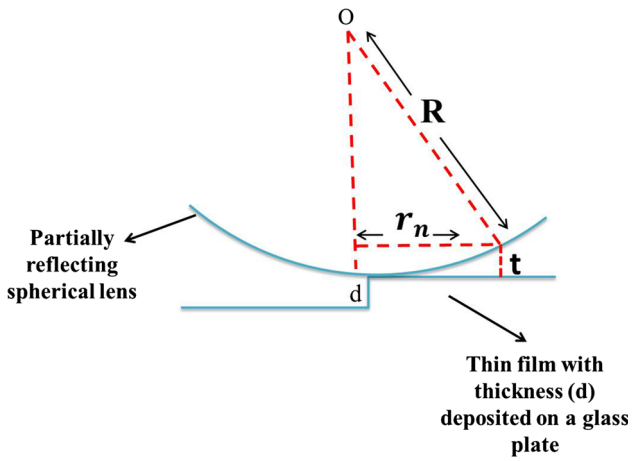

Fig. 2 A schematic diagram showing the used interferometer setup where a thin film is deposited on one half of the glass plate

line whose slope equals the radius of curvature R of the used spherical surface.

2.2. Sub-micrometric thin film's thickness determination

In this part, a thin film was deposited on half of the glass plate using the thermal evaporation technique. The lens's vertex was placed on the boundary between thin film and film-free regions. In this case, Newton's ring fringes were differently formed in these two regions; see Fig. 2. The presence of the film under the lens produced a step in the formed ring. Therefore, the condition of obtaining bright fringes through the larger air gap between the glass plate and lens's surface should be:

$$2(t(r) + d) = n\lambda \tag{6}$$

where d is the thin film's thickness.

Substituting Eq. (2) in Eq. (6), we get

$$\frac{(r_n)_g^2}{R} + 2d = n\lambda \tag{7}$$

where $(r_n)_g$ is the radius of the (nth) ring formed through the air gap between the glass plate and the lens.

Equation (7) can be rewritten as:

$$(r_n)_g^2 = n\lambda R - 2dR \tag{8}$$

Also, the condition of obtaining bright fringes through the film–lens air gap can be written as,

$$\frac{(r_n)_f^2}{R} = n\lambda \tag{9}$$

where $(r_n)_f$ is the radius of the (nth) ring formed through the air gap between the film and the lens.

So,

$$(r_n)_f^2 = n\lambda R \tag{10}$$

Subtracting Eq. (8) from Eq. (10), we get

$$(r_n)_f^2 - (r_n)_g^2 = 2dR \tag{11}$$

To get R, Eq. (10) is applied for the ring of the order $(n + 1)$.

So,

$$R = \frac{(r_{n+1})_f^2}{(n+1)\lambda} \tag{12}$$

Substituting Eq. (12) in Eq. (11), the film's thickness can be expressed as:

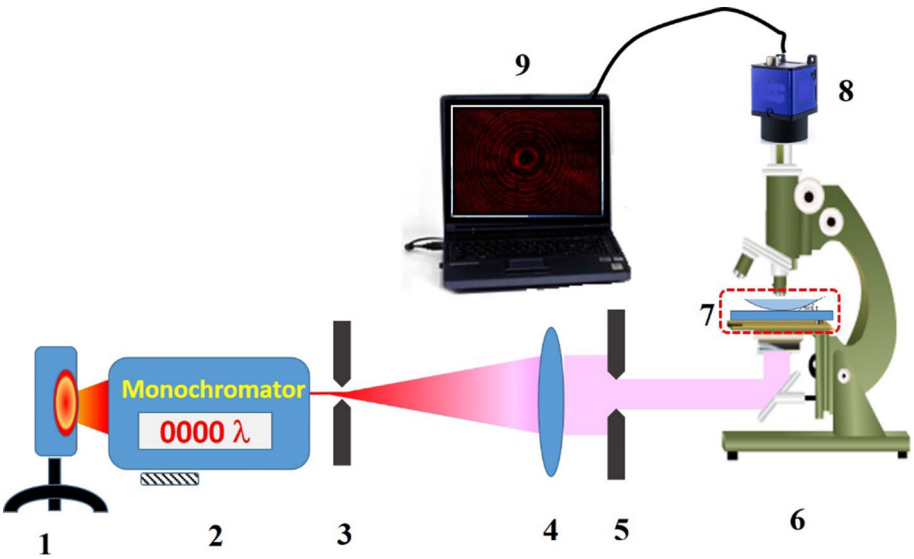

Fig. 3 Experimental setup. 1—Halogen lamp, 2—monochromator, 3—first diaphragm, 4—collimating lens, 5—second diaphragm, 6—optical microscope, 7—Newton's interferometer, 8—CCD camera, 9—PC computer

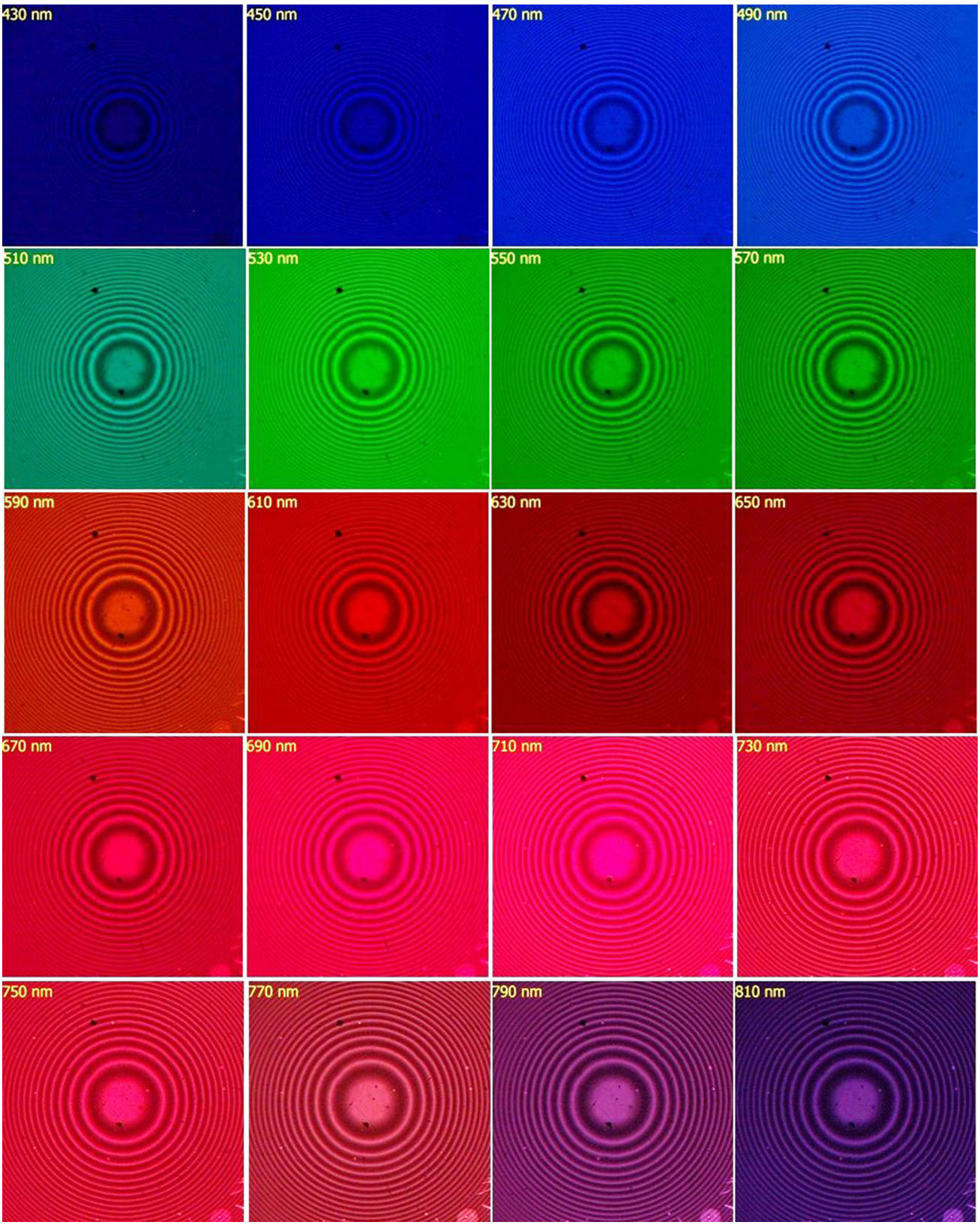

Fig. 4 A set of interference images corresponding to some wavelengths in the band (from 430 to 810 nm)

$$d = \frac{\left((r_n)_f^2 - (r_n)_g^2\right)(n+1)\lambda}{2(r_{n+1})_f^2} \quad (13)$$

From Eq. (13), we can determine easily and directly the thin film thickness by using the radii of the ring fringes through the film and film-free regions and the used wavelength.

3. Experimental setup

To achieve our aim, an optical arrangement is setup as shown in Fig. 3. In this setup, a halogen lamp (having visible and infrared continuous spectrum) was used. The emitted light was passed through a monochromator to select a desired wavelength and then passed through a diaphragm to adopt a spot of light. The produced monochromatic light was collimated using a convex lens to produce a parallel beam passing through another diaphragm and sent to be incident on the interferometer. The interferometer, spherical surface put on a glass plate, was placed on a microscope stage attached with a CCD camera, which in turn sent the interferograms to a PC computer for recording.

4. Results and discussion

4.1. Spherical radius retrieving

Using the previously illustrated experimental setup, a set of interference rings were recorded corresponding to some wavelengths in the band (from 430 to 810 nm); see Fig. 4. From these images, one can notice that the ring's radius for a certain interference order n increases by increasing the wavelength which verifies Eq. (4).

The prepared MATLAB software was used to analyze the recorded interference images and determine the bright rings radii r based on the intensity distribution of the fringes. A graphical relation between the wavelength and the squared value of the bright rings radii considering the magnification of our system was plotted for different fringes orders (from $n = 1$ to $n = 10$); see Fig. 5. Ten straight lines, each of them has a slope $m_n = (nR)$, were obtained. The radius of the spherical surface (R) was obtained by plotting another relation between the slopes (m_n) and the order (n) which gives a straight line with slope equals (R); see Fig. 6. The retrieved value of the radius of the used spherical surface was found to be (9.40 ± 0.08 cm). The determined value for the radius of curvature using a spherometer was 9.84 ± 0.40 cm. Moreover, we used the method presented by El-Zaiat [15] to calculate the radius of curvature of our surface. The radius was found to be 9.37 ± 0.34 cm.

4.2. Thin film thickness determination

Using the experimental arrangement shown in Fig. 2, some interferograms were recorded for two films with different thicknesses. Figure 7 shows a set of interferograms for the film (1) captured at three wavelengths (550, 580 and 610 nm). Using the prepared MATLAB software, these interferograms were analyzed to extract their intensity distributions and determine the rings radii. By measuring two successive rings' radii in the film–lens air gap interferograms and one ring radius in glass–lens air gap interferograms and applying Eq. (13), the mean thin film thickness was calculated from the interferograms of the three used wavelengths. Similarly, the thickness of a thicker film (2) was determined from three interferograms recorded at (436, 546 and 578 nm); see Table 1. From this table, one can notice that the proposed method is quite

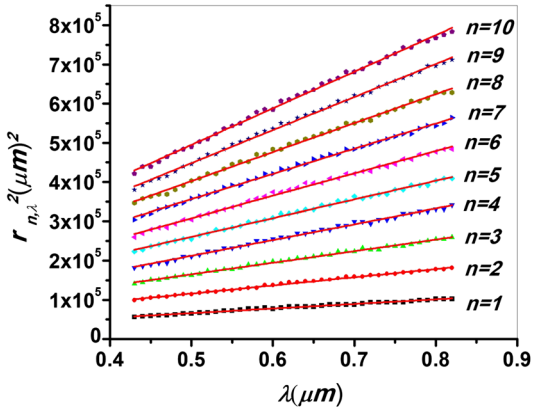

Fig. 5 Graphical relation between the wavelength and the bright rings' radii for different orders

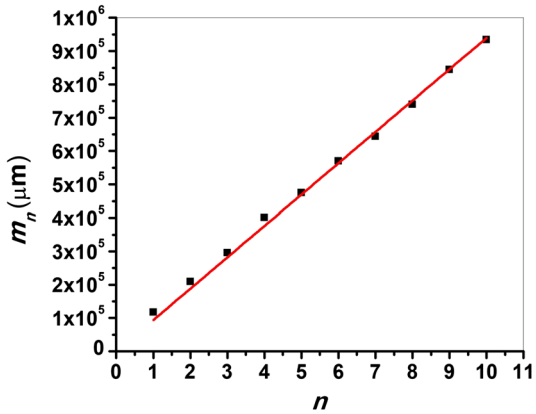

Fig. 6 Graphical relation between the slopes of the straight lines shown in Fig. 5 and the rings orders

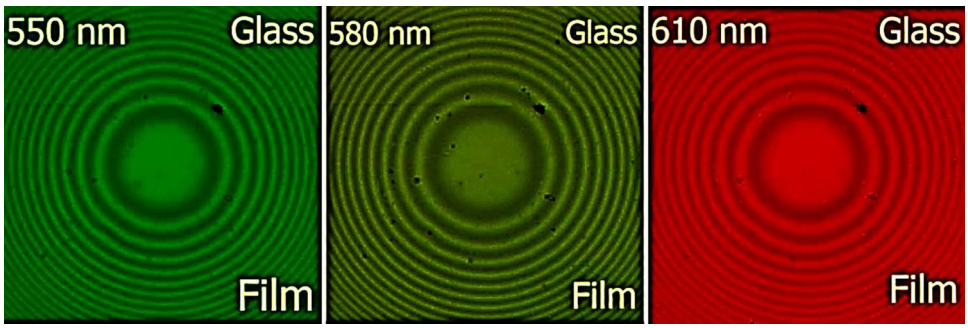

Fig. 7 A set of interference images for the film (1) with three wavelengths (550, 580, 610 nm)

Table 1 Film (1) and (2) thicknesses and their standard deviations

Film number	Wavelength (nm)	Thickness (nm)	Wavelength (nm)	Thickness (nm)	Wavelength (nm)	Thickness (nm)	Mean value of thickness (nm)	SD (nm)
Film 1	550	43.2	580	43.8	610	44.3	43.8	0.5
Film 2	436	101.4	546	100.2	596	102.9	101.5	1.4

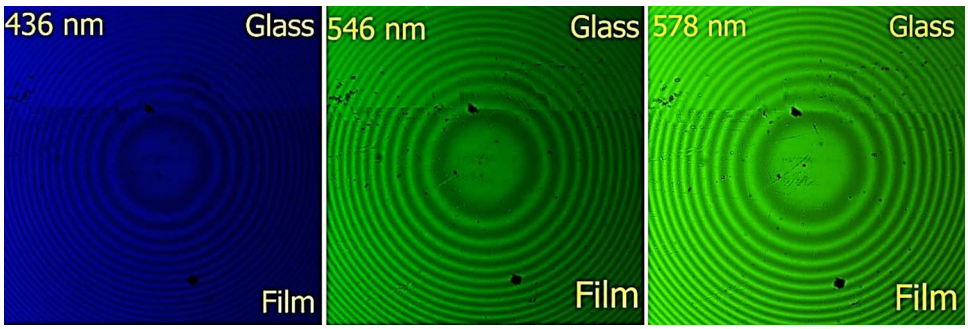

Fig. 8 A set of interference images for the film (2) with three wavelengths (436, 546, 578 nm)

accurate and direct with an error that does not exceed 1.4 nm for the film of thickness 101.5 nm and 0.5 nm for the film of thickness 43.8 nm. From these results, it is clear that the presented simple method was able to obtain a sub-micrometric thin film thickness with an accuracy in the order of nanometers (Fig. 8).

5. Conclusions

An attempt to retrieve a spherical radius using variable wavelength Newton's ring fringes formed in transmission is presented. The suggested method depends on the ring fringes radii variation with the variation of the wavelength of the illuminating source. A set of interferograms is recorded for wavelength variation from 430 to 810 nm. A MATLAB program is prepared for reading the interference image intensity distribution and then determining the radii of the bright fringes. A graphical relation between the wavelength and the squared values of fringes radii is plotted for different fringes orders. A set of straight lines is obtained. Another relation is plotted between the slopes of these straight lines and the fringes' orders. The radius of the used spherical surface is determined directly from the last graphical relation. The retrieved value of the spherical radius was found to be in a good agreement with that determined by other methods.

In addition, a method for sub-micrometric thin film measurement using Newton's rings in transmission is proposed. This method based on depositing the film on half of a glass plate. This plate and a partially reflecting lens construct the interferometer where the lens stands on the boundary between film and film-free regions. One can notice that there is a step in the obtained ring fringes due to the presence of the thin film. The previously prepared MATLAB program is used for the determination of the fringes radii. The thin film thickness is determined using the difference in the ring fringes radii in the film and the film-free regions. This method is applied for two films with different thicknesses. The measured values and the standard deviations listed in Table 1 show the nano-metric accuracy of the presented method.

References

[1] D Malacara, 3rd ed. (*John Wiley & Sons, Inc.*) 1 (2007)
[2] B Stern *Rev. Sci. Inst.* **34**(2) 152 (1963)
[3] C Gentle and M Halsall *Opt. Lasers Eng.* **3**(2) 111 (1982)
[4] L Dettwiller and P Chavel *Opt. Commun.* **54**(1) 1 (1985)
[5] M Medhat, A Hassan, N EL-Nashar and S Salman *Opt. Laser Technol.* **23**(5) 308 (1991)
[6] S Dubrovskii, M Lagutina and K Kazanskii *Polym. Gels Netw.* **2**(1) 49 (1994)
[7] A Podoleanu, G Dobre, D Webband and A Jackson *Opt. Lett.* **21**(21) 1789 (1996)
[8] C Illueca, C Vazquez, C HernaÂndez and V Viqueira *Ophthal. Physiol. Opt.* **18**(4) 360 (1998)
[9] L Goldner, J Hwang, G Bryant, M Fasolka, P P Absil, J V Hryniewicz, F G Johnson, H Shen and P-T Ho *Appl. Phys. Lett.* **78**(5) 583 (2001)
[10] K Wahl, R Chromik and G Lee *Wear* **264**(7–8) 731 (2008)
[11] K Raveesha, K Kumar and B Prasad *Int. Lett. Chem. Phys. Astron.* **48** 27 (2015)
[12] Z Yang, K Wang, J Cheng, Z Gao and Q Yuan *Appl. Opt.* **55**(17) 4769 (2016)
[13] J Wu, M Lu, R Tao, F Zhang and Y Li *Opt. Lasers Eng*. **91** 178 (2017)
[14] W A Ramadan, H H Wahba *Appl. Phys. B* **124**(2) 1 (2018)
[15] S Y El-Zaiat *Pure Appl. Opt.* **4**(5) 469 (1995)